Local moment disorder in ferromagnetic alloys

H. Akai
Department of Physics, Nara Medical University, Kashihara, Nara 634, Japan

P. H. Dederichs
Institut für Festkörperforschung, Forschungszentrum Jülich, D5170 Jülich, Germany
(Received 19 October 1992)

Local moment disorder, defined as a random arrangment of two distinct magnetic states of the same atomic species in a metallic system, is discussed in the framework of the Korringa-Kohn-Rostoker coherent-potential approximation combined with the local-density-functional method and applied to Fe-Cr, Ni-Fe, and Ni-Mn alloys. For Fe-Cr alloys it is found that the disordered-moment state has a higher energy than the ferromagnetic state in the entire region of Fe concentrations. Thus the theory fails to explain the spin-glass state observed around $Fe_{0.14}Cr_{0.86}$. The theory, on the other hand, can explain the transition of Ni-Fe alloys from ferromagnetism to paramagnetism around the Invar region; the transition, however, is of first order, in contrast to experimental indications. The volume contraction due to the reversal of the magnetic-moment alignment from parallel to antiparallel with respect to the bulk magnetization is also discussed in connection with the Invar anomalies. For Ni-Mn alloys the calculation shows that, when the Mn concentration is larger than 15 at. %, magnetic states with local moments parallel and antiparallel to the average magnetization coexist even in the ferromagnetic region. The results are quite consistent with NMR experiments, which clearly show the existence of the antiparallel Mn local moments in addition to the parallel ones.

I. INTRODUCTION

It is well known that local magnetic properties of magnetic transition-metal alloys often strongly depend on the local environment. For example, experiments tell us that the local magnetic moment of Fe atoms in Fe-Co alloys varies from 2.2 to $3\mu_B$ depending on the number of their nearest neighboring Co atoms.[1] Such a variation in the local magnetic properties, however, usually plays only a minor role in determining the bulk properties observed experimentally.[2] This means that the single-site effective medium theory such as the coherent-potential approximation (CPA) works satisfactorily in most cases. Exceptional cases are systems with large local magnetic moments which can have some different but energetically almost degenerate orientations. In a single-site treatment, we may classify these orientations as either parallel or antiparallel to the average magnetization since a canted local moment is quite unlikely in this case.[3] A Mn atom in Ni-Mn alloys is a typical case. A Mn atom isolated from other Mn atoms will align its local magnetic moment towards the bulk magnetization. On the other hand, when two Mn atoms come closer, there is a tendency for antiparallel coupling between the local magnetic moments. As a result, the local magnetic moments shows a broad orientational distribution with more or less the same absolute value of the moment. In this case a naive averaging over the constituent atoms in the effective medium as in the CPA will fail to give a good description of the average properties. The situation is easily understood by considering the case where the bulk magnetization becomes zero: CPA will give a vanishing local magnetic moment for the Mn atoms, but in reality have different orientations, so that only the average moment vanishes. Since the magnetic energy is quadratic with respect to the local moment, this effect does not average out in the energy and is important for many physical properties, e.g., the proper lattice constant of the alloys.

In this paper we develop a first-principles method that is compatible with such static magnetic fluctuation (magnetic disorder) mentioned above. The basic idea is that we may treat such systems by introducing a fictitious many-component system. The approach is first proposed by Jo for Ni-Mn systems;[4,5] he introduced a pseudoternary alloy, $Ni_xMn_{\uparrow y}Mn_{\downarrow z}$, instead of Ni_xMn_{1-x}, and minimized the total energy with respect to y, or equivalently z, for given concentration x of Ni atoms. In that time he used tight-binding CPA combined with the Hartree-Fock appproximation (HF-TB-CPA).[6] The main purpose of the present paper is to apply such an attempt to Korringa-Kohn-Rostoker coherent-potential approximation (KKR-CPA) combined with the local spin-density formalism (LSD),[7,8] and thus to enforce this powerful method for disordered systems.

Let us first look into the method briefly. Suppose a Mn atom, for instance, is embedded in an effective CPA medium. For Ni-Mn systems, two LSD solutions are possible for the Mn impurity in the medium, $Mn_\uparrow$ and $Mn_\downarrow$. This can happen when the valence of the solute atom is not very far from half filling, like Mn. This, however, does not mean that the two kinds of Mn atom coexist in the system. One of the two atomic states in general has a lower formation energy than the other, which prevents the appearance of the second Mn configuration with the higher formation energy; the coexistence occurs only when the formation energies of both configurations

become equal. This last condition is delicately affected by the filling of the effective medium or, in other words, the concentration of constituent atoms.

For Ni-Mn systems, the coexistence of two magnetic states does not occur in the low Mn concentration region ($x_{\mathrm{Mn}}<0.1$); the formation energy of $\mathrm{Mn}_{\downarrow}$ is larger than that of $\mathrm{Mn}_{\uparrow}$ so that all the Mn atoms should be $\mathrm{Mn}_{\uparrow}$. With increasing Mn concentration, however, the average electron number decreases and at a certain Mn concentration, the formation energies of the two states become equal. By further increasing the Mn concentration, the coexistence of $\mathrm{Mn}_{\uparrow}$ and $\mathrm{Mn}_{\downarrow}$ is possible. The concentration of both types of Mn is determined in such a way that the formation energies of these states are exactly equal; this is nothing but the energy minimum requirement.

In the following sections we will demonstrate that the above treatment gives qualitatively very different results from the ones obtained by the usual KKR-CPA for Ni-Mn and Ni-Fe systems near the magnetic transition. For the former, we show that the coexistence of two magnetic states is realized even in its ferromagnetic region. The situation is consistent with the experimental observation reported by Kitaoka and Asayama[9] and Kitaoka, Ueno, and Asayama.[10] They found ^{55}Mn NMR signals distributed in the low-frequency region for Ni-Mn alloys in addition to those already known in a higher-frequency region, confirming that they originated from antiparallel alignments of Mn local magnetic moments to the magnetization.

As for the Ni-Fe system, Kanamori, Teraoka, and Jo pointed out[11] that within a reasonable choice of the parameters the tight-binding model reproduced the magnetic behavior near the transition from ferromagnetism to paramagnetism. They suggested that the deviation of the magnetization from the linear dependence on Fe concentration (Slater-Pauling curve) near the Invar region might be due to quantum-mechanical (dynamical) fluctuation of Fe spin and that the situation could be partly describable by the appearance of $\mathrm{Fe}_{\downarrow}$ in the Ni-Fe matrix. Our result, however, is slightly different; the transition from ferromagnetism to paramagnetism is rather sudden and no intermediate states where the ferromagnetism is weakened by the existence of $\mathrm{Fe}_{\downarrow}$ are realized.

We briefly summarize the theoretical framework in Sec. II. The results are presented and discussed in Sec. III. Section IV is devoted to the summary and supplementary discussions. Some details about the calculation are described in the Appendix.

II. KKR-CPA-LSD WITH MULTIPLE LOCAL MAGNETIC STATES

For a given chemical composition $A_{1-x}B_x$ of AB alloy, we can introduce additional degrees of freedom corresponding to the magnetic components for each chemical component such as $A_{\uparrow s}A_{\downarrow t}B_{\uparrow u}B_{\downarrow v}$, where $s+t=1-x$ and $u+v=x$. We can deal with such systems as a four-component alloy in the framework of usual KKR-CPA-LSD. Though systems so far treated by KKR-CPA-LSD have been mostly binary, the application of the method to many-component systems is trivial. A brief summary of KKR-CPA-LSD, together with the expression of the total energy used below, is given in the Appendix. Here we suppose that we obtained the self-consistent solution (in the sense of both CPA and LSD) of this four-component system with given concentration s, t, u, and v. In many cases, the two magnetic states, $A_{\uparrow}$ and $A_{\downarrow}$, or those for a B atom, actually are not stabilized, i.e., only a single magnetic state can be a local solution of the Kohn-Sham equation of LSD for the atoms under consideration. However, when two distinct magnetic states appear for one (or both) of the chemical components, further minimization of the total energy with respect to s and u is a reasonable way to determine the concentration of the magnetic components:[4]

$$dE/ds=0 \ , \quad \text{and} \quad dE/du=0 \ , \tag{2.1}$$

where $E(s,t,u,v)$, whose expression is given in the Appendix, is the total energy compatible with LSD. The above equations may be simplified by taking account of the variational properties of LSD and CPA, i.e.,

$$\delta E/\delta\rho=0 \ , \quad \text{and} \quad \delta E/\delta\tilde{t}=0 \ , \tag{2.2}$$

where ρ is the charge (spin) density and $\tilde{t}$ is the coherent t-matrix describing the effective CPA medium (see the Appendix). The first equation is a direct consequence of LSD and the second one is due to the CPA self-consistency,[12] which can be shown rigorously for the band energy given in the Appendix (note that the argument, however, is somewhat artificial since the second condition is satisfied only for the band energy of functional form implied by (A2.2) and (A2.4), which of course is not unique.) Combining (2.2) and (2.1), we finally obtain

$$\partial E/\partial s=\partial E/\partial t \ , \quad \text{and} \quad \partial E/\partial u=\partial E/\partial v \ . \tag{2.3}$$

The above condition requires that the formation energy for parallel and antiparallel moment alignments are equal, thus determining the correct concentration s or u, respectively.

Now let us look into the possibility of finding out the solution of (2.1) following the discussion by Jo and Miwa.[4,5] In general the situation has nothing to do with the chemical disorder and we tentatively suppose that the system is pure and specified with effective d electron filling Z. Also we assume that the system has more-than-half-filled d bands as is the case of typical ferromagnetic Fe- or Ni- based alloys. The behavior of magnetic impurities located in this system is the following: If the host system is paramagnetic (or nonmagnetic), three different LSD solution are possible, one unstable with a vanishing moment, two stable solutions with local moment $\pm M$. The situation is illustrated in Fig. 1. If the host system becomes ferromagnetic, the curves corresponding to the solution are deformed and connected into a single S-shaped curve (see Fig. 1). The energy variations along the path of varying (z component of) local magnetic moment m are also illustrated in Fig. 1. In the ferromagnetic host, impurities with more-than-half-filled d electrons prefer parallel coupling to the host magnetization, and those with less-than-half filled prefer antiparallel coupling (the situation would be reversed for less-

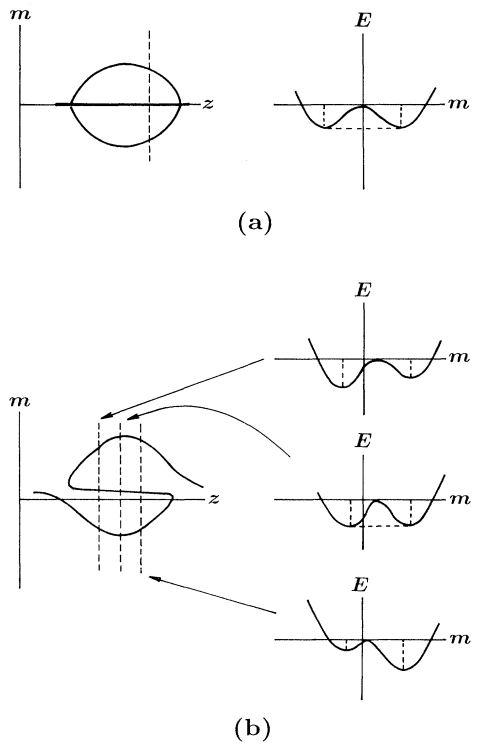

FIG. 1. Local magnetic moments obtained by LSD as a function of impurity valence Z; (a) in a paramagnetic host, (b) in a weakly ferromagnetic host. Also shown (right-hand side) are the changes in the total energy with varying magnetic moment along the path indicated by the dashed lines of the corresponding m vs Z curves in the left. The crossover, which occurs with increasing impurity valence, from antiparallel to parallel coupling of the local impurity moment to the host magnetization is sketched.

than-half-filled host bands). For a certain filling of the impurity d electrons the crossover from the parallel to the antiparallel coupling takes place. At the crossover, the two local states have the same formation energy, giving rise to the possibility of coexistence of two different magnetic states.

The same may happen even if the host and the impurity atoms are chemically equivalent. In this case the above procedure has to be used to construct an effective medium as host system in the sense of the mean-field theory; first take a weighted average of the parallel and the antiparallel solution at the impurity site and then introduce this as effective scattering centers at the host sites. The weight is determined such that the system becomes totally self-consistent, i.e., the formation energy of the two magnetic states becomes equal.

The situation admittedly is not very realistic for pure or ordered systems since in these systems magnetic ordering such as antiferromagnetism or ferrimagnetism will occur. For disordered systems, however, the local magnetic moments more or less fluctuate from site to site depending on the local environment, and a statistical treatment of such local properties is rather realistic. Moreover, since the average filling of d band can be now continuously changed as a function of the concentration of component atoms, multiple local magnetic configurations are easily attainable. In the following section we will examine such a possibility by taking both chemical and magnetic disorder into account.

III. RESULTS

Actual minimization of the total energy with respect to the concentration of the magnetic component is performed by direct comparison of the calculated total energies for various concentrations. Alternatively we may calculate the formation energy of each component and see if they satisfy the condition implied by (2.1); in principle this will be less expensive from a computational point of view. In reality, however, the first method yields more reliable results. Namely, the latter requires much higher accuracy due to linear dependence of the formation energy on the charge and spin densities, whereas it is quadratic for the former in the vicinity of the self-consistent solution. The minimization with respect to the lattice constant is indispensable since the magnetovolume coupling sometimes plays a critical role in the determination of the ground-state magnetic structure. KKR-CPA-LSD was performed in the way described in Ref. 13, the scalar relativistic treatment[14,15] was employed, and either the von Barth-Hedin LSD expression[16] with the Moruzzi-Janak-Williams parametrization[17] or the expression by Vosko-Wilk-Nusair[18] was used; the results were not much dependent on the choice of the LSD scheme.

A. Fe-Cr

Pure Cr is an antiferromagnet with an incommensurate spin-density wave. In the phase diagram of Fe-Cr, the antiferromagnetic phase is stable up to ~ 14 at. % Fe, where the antiferromagnetic-to-ferromagnetic transition takes place. Experiments reveals that in a narrow region in between these two magnetic phases a spin-glass phase exists.[19–23] Our central interest is whether the spin-glass phase observed in this system corresponds to the local-moment disordered states discussed in this paper. Our calculation shows that in addition to the ferromagnetic state the local-moment disordered state with no net magnetization exist as a stable solution in the entire range of Fe concentration for this system. Figure 2 plots the energy difference between two magnetic states; the local-moment disordered state always has a higher energy than the ferromagnetic state. The energy difference is around 10 mRy for pure iron (corresponding to the Curie temperature of Fe, roughly speaking) and becomes zero at pure Cr, which is nonmagnetic in the present treatment (antiferromagnetic ordering is not considered here). In the magnetic disordered state, the local magnetic moment at the Cr site vanishes, only the Fe sites being magnetic with a magnetic moment of around $\pm 1.7\mu_B$. Calculated values of the total-energy, local magnetic moment at each site, and the magnetization, all for $Fe_{0.2}Cr_{0.8}$, are given in Table I. Our initial expectation was that at low Fe concentration the local-moment disordered state would lie energetically below the ferromagnetic state en-

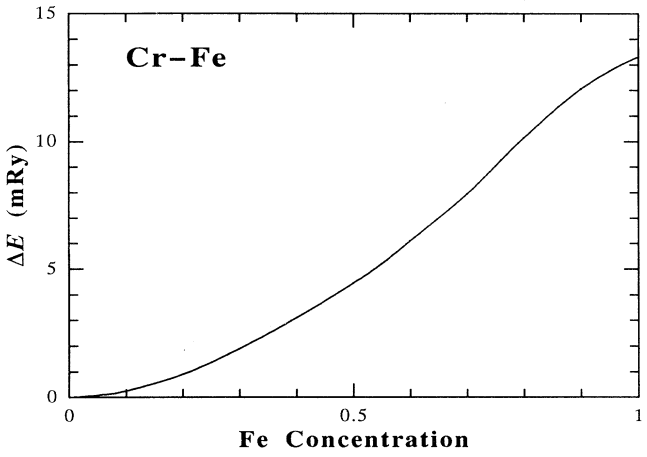

FIG. 2. Total energy of the local-moment disordered state of Fe-Cr relative to that of the ferromagnetic state vs Fe concentration.

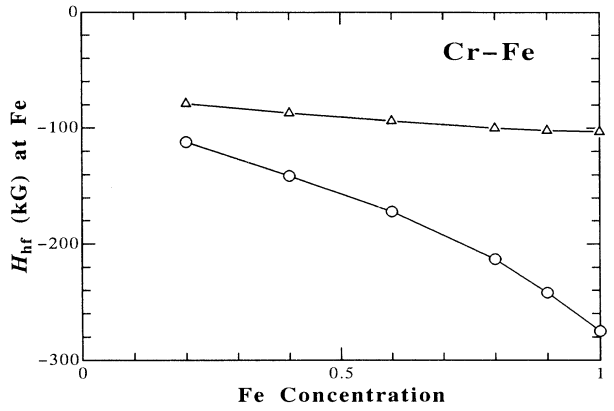

FIG. 3. Calculated hyperfine fields of Fe vs Fe concentration in the ferromagnetic state (circles) and the local-moment disordered state (triangles).

ergetically. Instead, the opposite is true: Due to the complete disorder, Cr sites lose the local magnetic moment entirely, gaining no exchange energy, and push up to the total energy of the magnetic disordered state relative to that of the ferromagnetic state. We conclude thereby that the observed spin-glass state might be explained only by taking account of the short-range antiferromagnetic correlation between Cr atoms as well as the effects beyond the single-site treatment of CPA.

The present results are different from those implied by Jo,[24] who concluded that, in the framework of HF-TB-CPA, the local-moment disordered state could be realized in this system. He pointed out, however, that the result was rather sensitive to the choice of the parameter controlling the intra-atomic Coulomb energy of an Fe atom. The corresponding LSD quantity seems somewhat bigger than assumed by Jo, which stabilizes the ferromagnetic state in the entire region of Fe concentration.

It might be worthwhile, however, to present some local quantities which depend on the local magnetic states. This may be meaningful since the spin-glass state obviously resembles the present disordered state locally, irrespective of the energetics obtained by the calculation. Figures 3 and 4 show the hyperfine fields and the isomer shifts at the Fe site, respectively. For the isomer shift the calibration constant of -0.24 (a.u. volume mm/sec) consistent with our previous impurity calculation[25] is used. Two curves in each figure correspond to the two different magnetic states; a branching from ferromagnetic to disordered values should occur when the concentration of Fe decreases down to around 20%.

TABLE I. Calculated total energy E, lattice constant a, and the local magnetic moments at Fe and Cr sites, m_{Fe} and m_{Cr}, respectively, in the ferromagnetic (F) and the local-moment disordered (LMD) states of $Fe_{0.2}Cr_{0.8}$.

	E (Ry)	a (a.u.)	m_{Fe} (μ_B)	m_{Cr} (μ_B)
F	−2186.329 95	5.2944	1.867	~0
LMD	−2186.329 90	5.2945	±1.432	0

B. Ni-Fe

For this system, we shall concentrate on the ferromagnetic-to-paramagnetic transition, which takes place near the Invar region (~60 at. % Fe). Our previous calculation showed that, in the single-site treatment, a first-order-like transition from ferromagnetism to nonmagnetism occurred when we increased the Fe concentration.[26,27]

Figure 5 shows the total energy of the systems for various Fe concentrations as functions of the ratio $C_{Fe\downarrow}/C_{Fe\uparrow}$, where $C_{Fe\downarrow}$ and $C_{Fe\uparrow}$ are the concentrations of $Fe_\downarrow$ and $Fe_\downarrow$ atoms, respectively. The results indicate that for the Fe concentration less than ~60% the energy minimum corresponds to the pure ferromagnetic states, i.e., no Fe atoms with down magnetic moments appear.

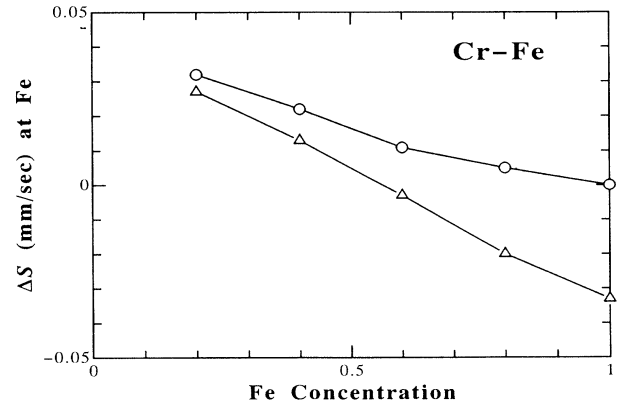

FIG. 4. Calculated isomer shifts of Fe vs Fe concentration in the ferromagnetic state (circles) and the local-moment disordered state (triangles).

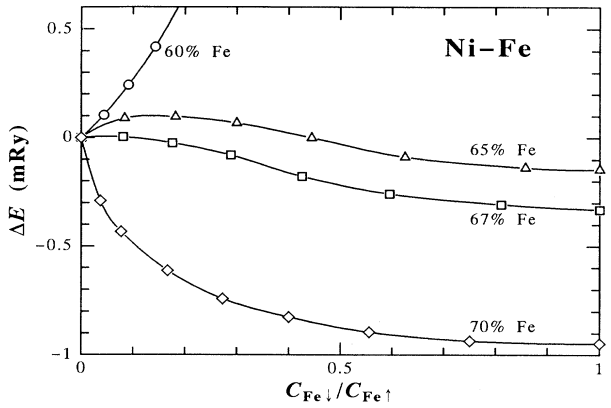

FIG. 5. Total energy of the local-moment disordered state relative to that of the ferromagnetic state as a function of $C_{Fe\downarrow}/C_{Fe\uparrow}$ of $Ni_{1-x}Fe_x$ for $x=0.6$ (circles), 0.65 (triangles), 0.67 (squares), and 0.7 (diamonds). The lattice constant is determined by energy minimization.

On the other hand, the energy minimum for the system with Fe concentration more than ~65% corresponds to the paramagnetic states with $C_{Fe\downarrow}=C_{Fe\uparrow}$. The transition from ferromagnetism to paramagnetism is of first order as a function of the concentration. This last point is somewhat delicate. Figure 6 shows a similar plot but calculated for a fixed lattice constant. The results wrongly suggest a second-order-like transition.

Experimentally the transition seems to be rather gradual. At present we do not want to discuss the possible origin of this discrepancy between the theory and the experiments simply because the experimental situation is not so clear due to possible inhomogenieties and due to the phase separation associated with the fcc-bcc martensitic transformation.

Table II compares some local quantities together with the total energy and the equilibrium lattice constant of ferromagnetic, nonmagnetic, and the local-moment disordered states, all for $Ni_{0.35}Fe_{0.65}$ as a typical case. For this system, the nonmagnetic state has the highest total energy, the local-moment disordered state the lowest one. The usual KKR-CPA-LSD treatment would predict the ferromagnetic state as the ground state in this case. In the present calculation the magnetic transition takes place in between $x=0.6$ and 0.65, where x is the Fe concentration. At the transition point, the average magnetization will jump from $\sim 1.8\mu_B$ to zero, and the magnitude of the local magnetic moment at the Fe site, from $\sim 2.4\mu_B$ to $\sim 1.7\mu_B$. Correspondingly the hyperfine field at Fe nuclei changes from around −290 kG to ±87 kG (in comparing these values with experiments, it should be noticed that the hyperfine field of Fe is always underestimated in LSD by 20 to 30% Ref. 28. To the authors' knowledge, no experimental hyperfine fields corresponding to this situation have been reported.

TABLE II. Calculated total energy E, lattice constant a, bulk magnetization M, and the local magnetic moments of Fe and Ni, m_{Fe} and m_{Ni}, respectively, in the ferromagnetic (F), nonmagnetic (NM) and the local-moment disordered (LMD) states of $Ni_{0.35}Fe_{0.65}$.

	E (Ry)	a (a.u.)	M (μ_B)	m_{Fe} (μ_B)	m_{Ni} (μ_B)
F	−2714.469 49	6.6653	1.809	2.365	0.736
NM	−2714.469 38	6.4807	0	0	0
LMD	−2714.469 84	6.5295	0	±1.668	0

The difference in the lattice constant among three magnetic states is obtained from the lattice constants given in the table. The striking feature is that the difference between the ferromagnetic and the local-moment disordered state is much bigger than that between paramagnetic and the local-moment disordered states. Since the local magnetic energy between the ferromagnetic and the local-moment disordered state can not be much different (Fe local magnetic moments of the two systems are rather similar), this difference must originate from the gain in the band energy for the latter. In other words, the single-site magnetovolume effect cannot explain the lattice expansion of the system. This observation is quite consistent with the results obtained many years ago by Kanamori, Teraoka, and Jo[11] and Kanamori and Teraoka,[29] who studied the mechanism underlying the Invar effects by use of the interacting virtual-state approach.[11,29]

Now, let us briefly discuss the finite temperature properties of this system in connection with the Invar anomalies. Though the present approach intends to describe the local-moment disordered state introduced by local environments, its application to thermal disorder might also be conceivable;[30–33] such approach corresponds to the saddle-point and the static approximation of the functional integral approach for the finite temperature magnetism. In the ferromagnetic region, the finite temperature properties are governed by the magnetic excitation which reverses the local magnetic moment. The situation somehow resembles the magnetic disorder discussed above. This allows us to pursue the following argument: Though the single-ion contribution to the

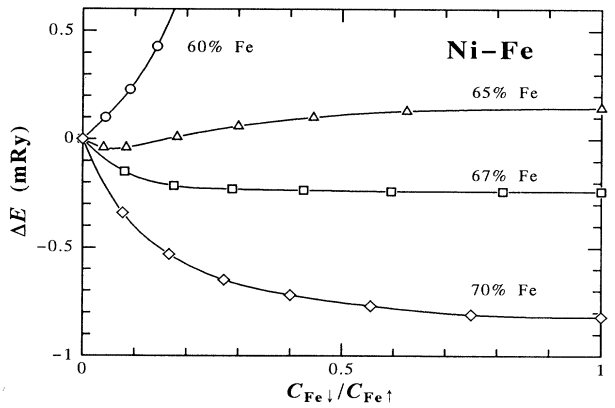

FIG. 6. Same plot as Fig. 4 but the lattice constant is fixed to that of $Ni_{0.4}Fe_{0.6}$ in this case. The transition from the ferromagnetic to paramagnetic states is now gradual.

volume does not change much with elevating temperature, change in the ion-ion coupling due to the magnetic disorder greatly reduces the volume of the system as observed above. The relation of the present picture to Weiss's two-γ-state model[34] is not quite clear. However, we may say that the physical situation assumed in Weiss's model is seemingly not very different from the present one.

We expect that a quantitative discussion of the Invar anomalies based on first-principles electronic structure calculations may be possible along the line implied by the present approach.

C. Ni-Mn

Among others, Ni-Mn is a typical example for which the existence of parallel and antiparallel magnetic states was evidenced by NMR experiments.[9] Stimulated by Jo's prediction,[4] Kitaoka and Asayama,[9] and Kitaoka, Ueno, and Asayama[10] performed intensive NMR study on Ni-Mn and found ^{55}Mn NMR signals ranging 140–180 MHz in addition to 260–360 and 330–400 MHz that had been already known. From the shift of the signals caused by the applied external field they concluded that the new signals correspond to those Mn moments which couple antiparallel to the bulk magnetization.

The main purpose of our calculation is to confirm the existence of such a magnetic state in the framework of LSD and also to give some quantitative results, especially for the hyperfine field distribution.

Figure 7 shows the total-energy change of $Ni_{0.85}Mn_{0.15}$ and $Ni_{0.80}Mn_{0.20}$ as functions of $C_{Mn\downarrow}/C_{Mn\uparrow}$. The energy minimum occurs around $C_{Mn\downarrow}/C_{Mn\uparrow}=0.25$ for $Ni_{0.85}Mn_{0.15}$ and around 0.5 for $Ni_{0.80}Mn_{0.20}$, meaning that the systems are still ferromagnetic, but that not all the local magnetic moments align parallel to the magnetization. Thus, the transition from ferromagnetism to paramagnetism is gradual in this system. The calculated magnetization as a function of the Mn concentration is compared with experiments in Fig. 8. One might argue that the calculation based on the usual KKR-CPA-LSD with a single magnetic state can as well reproduce the observed magnetization, at least qualitatively.[26,27] It is clear, however, that the physical situations considered by the two methods are very different. It also shows that the usual CPA describes average quantities like the average magnetization quite well, even when the microscopic model is not very realistic.

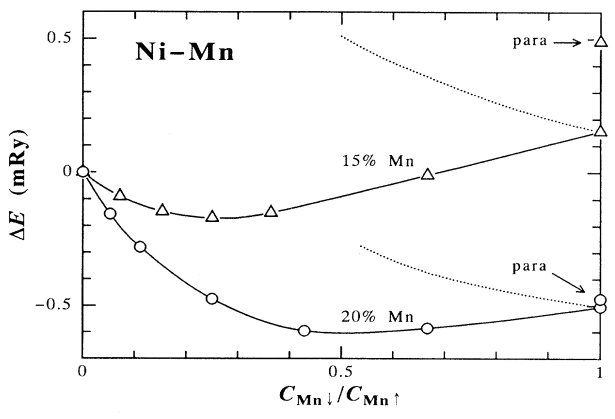

FIG. 7. Total energy of the local-moment disordered state relative to that of the ferromagnetic state as a function of $C_{Mn\downarrow}/C_{Mn\uparrow}$ of $Ni_{1-x}Mn_x$ for $x=0.15$ (triangles) and 0.2 (circles). Dotted lines correspond to the solution with a negative magnetization (in other words, $C_{Mn\downarrow}/C_{Mn\uparrow}>1$ with a positive magnetization), the arrows indicate the paramagnetic solution, i.e., local-moment disorder with vanishing net magnetization ($C_{Mn\downarrow}/C_{Mn\uparrow}=1$ does not necessarily mean the paramagnetism).

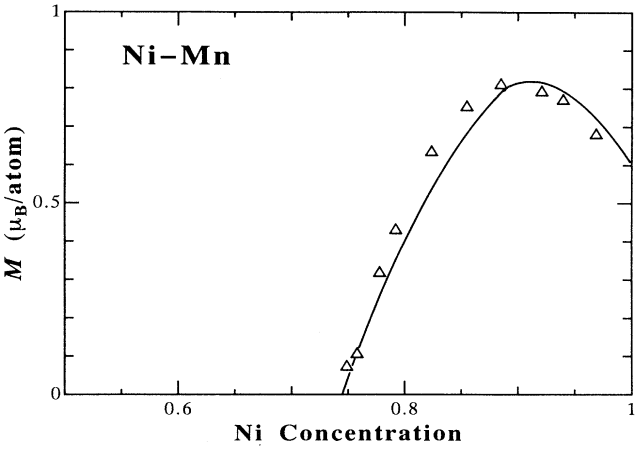

FIG. 8. Magnetization of the Ni-Mn system vs Ni concentration (solid line) is compared with experiments (triangles). Experimental values from Ref. 35.

Table III lists detailed values of the magnetizations, local magnetic moments, and the hyperfine fields of these systems at their energy minima together with those obtained by usual KKR-CPA-LSD. Though the magnetization calculated by usual CPA already shows deviation from the linear increase with increasing Mn concentra-

TABLE III. Calculated magnetizations M, local magnetic moments, m_{Ni} and the m_{Mn}, and the hyperfine fields H_{hf} at Mn site of $Ni_{1-x}Mn_x$. The values obtained by usual KKR-CPA with a single magnetic state (ferromagnetic state) for $x=0.15$ are also given. As a result of the scalar relativistic treatment, the magnetization seems somewhat bigger than that obtained by nonrelativistic calculations, e.g., $0.618\mu_B$ of pure Ni is compared with the nonrelativistic value of $0.59\mu_B$ (Ref. 17). F, LMD, and P denote ferromagnetic, local-moment disordered, and paramagnetic (that is local-moment disorder with no net magnetization) states, respectively.

x	M (μ_B)	m_{Ni} (μ_B)	m_{Mn} (μ_B)	H_{hf}^{Mn} (kG)
0 (F)	0.618	0.638	2.78	−184
0.1 (F)	0.808	0.623	2.59	−189
0.15 (F)	0.840	0.596	2.34	−179
0.15 (LMD)	0.65	0.530	2.43, −2.34	−172, 50
0.2 (LMD)	0.41	0.341	2.25, −2.24	−140, 70
0.25 (P)	0	0	±2.15	±100

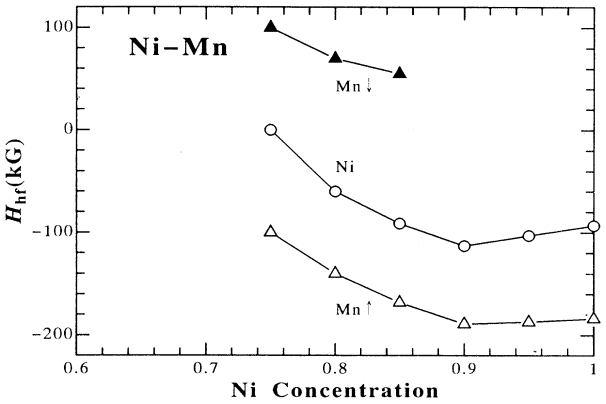

FIG. 9. Calculated hyperfine fields of Ni (circles), $Mn_{\uparrow}$ (open triangles), and $Mn_{\downarrow}$ (solid triangles) of Ni-Mn.

tion, at the low Mn concentration region (see Table III), the deviation is much less pronounced than the experimental observation (see Fig. 6). The present multiple-magnetic-state treatment, on the other hand, reproduces the experimental tendency quite well. This fact seems to indicate the importance of the static fluctuation of the local magnetic moments.

Figure 9 shows the expected hyperfine fields at the Mn nuclei. Corresponding to the appearance of the second magnetic solution, a hyperfine field of about +60 kG shows up in addition to the field of −160 kG at ~15 at. % Mn. The centers of the observed NMR frequencies on Mn nuclei in this system correspond to fields of ~ +160 kG for the antiparallel Mn and ~−290 and ~−345 kG for the parallel Mn. The fact that the present theory underestimates the Mn hyperfine fields by nearly half does not mean the theory fails in describing the valance electronic structure of the systems. Actually it is well known that LSD largely underestimates the core polarization contribution to the hyperfine fields when the d shell is strongly polarized.[28] From the comparison with the experiments for impurity systems, the deviation by about a factor of 2 for Mn atoms looks fairly reasonable.

In conclusion, for the Ni-Mn system, and presumably also for similar systems such as Fe-Mn and Fe-V,[36] as well as Ni-Co-Mn and Ni-Fe-Mn,[10] the present treatment of the multiple magnetic states well simulates local environment effects, which otherwise would be very difficult to treat from the first principles.

IV. SUMMARY

We present the results of generalized KKR-CPA-LSD calculation in which the possibility of local-moment disorder is considered. As typical cases, we have treated the Fe-Cr, Ni-Fe, and Ni-Mn systems. For Fe-Cr we concluded that the spin-glass phase observed experimentally could not be stabilized energetically as a disordered magnetic system. We nevertheless put emphasis on the usefulness of the present approach even for such cases since it enables us to deal with microscopic local quantities such as hyperfine fields and the isomer shifts of the spin-glass phase based on the first principles.

For the Ni-Fe system the magnetic transition around 65 at. % Fe was described in the present treatment as a transition from ferromagnetism to the local-moment disordered state. As for the invar anomalies, we pointed out that the existence of reversed local magnetic moments could be important in discussing the anomalies at finite temperatures. Such an aspect actually has been discussed many times from various different points of view. The essential point, however, can most likely be described by a static treatment like the present one. The advantage of the KKR-CPA-LSD is that the magnetovolume effects are automatically included, thus providing a straightforward method for a quantitative analysis of the Invar anomalies on a first-principles basis.

The most successful example may be the Ni-Mn system, for which the existence of two magnetic states with opposite direction of local magnetic moments even in the ferromagnetic phase is demonstrated. The calculated magnetization and the hyperfine field distribution are in reasonable agreement with experiments. The application of the present method to other systems with stable local moments, which nevertheless show magnetic instabilities, such as Fe-Mn or Ni-Co-Mn, for instance, and presumably Fe-Al,[37] would be interesting.

ACKNOWLEDGMENTS

Discussions with Professor T. Jo are greatly appreciated. The present work was partly supported by Grant-in-Aid for Scientific Research of Priority Area, Japanese Ministry of Education, Science, and Culture.

APPENDIX: TOTAL ENERGY IN KKR-CPA-LSD

1. Summary of KKR-CPA

First we briefly summarize KKR-CPA. Consider a n-component system $A_1 A_2 \ldots A_n$, where A_1, A_2, etc. denote the component atoms, with $x_1, x_2, \ldots, x_n$ being their concentrations. The backscattering part of the site-diagonal Green's function on each site of atom i in the CPA medium is then given by

$$G^i_{LL'} = \sum_{L''} \tilde{G}^{00}_{LL''}[1-(t_i-\tilde{t})\tilde{G}^{00}]^{-1}_{L''L'} , \tag{A1}$$

where t_i and $\tilde{t}$ are the single-site t matrix of atom i and of the effective CPA medium, respectively, and

$$\tilde{G}^{00}_{LL'} = \int_\tau \frac{d\mathbf{k}}{\tau} \tilde{G}_{LL'}(\mathbf{k}) = \int_\tau \frac{d\mathbf{k}}{\tau} \sum_{L''} g_{LL''}(\mathbf{k})[1-\tilde{t}g(\mathbf{k})]^{-1}_{L''L'} , \tag{A2}$$

with g being the free space structure Green's function. The integration with respect to $\mathbf{k}$ in the last expression is performed within the first Brillouin zone of volume τ. Now the CPA prescription determining $\tilde{t}$ is

$$\sum_i x_i G^i_{LL'} = \tilde{G}^{00}_{LL'} . \tag{A3}$$

2. Total-energy expression

The total energy of the system is calculated in the following way: First we decompose it into several parts

$$E_{\text{total}}=E_{\text{band}}-E_{\text{pot}}+E_{\text{stat}}+E_{\text{xc}} . \tag{A4}$$

To calculate the band energy, we introduce a function $Z(E)$, imaginary part of which gives the total number of states (per atom) below a real energy E:

$$Z(E)=\int_{\tau}\frac{d\mathbf{k}}{\tau}\{\ln\det|-E+(\mathbf{k}+\mathbf{g})^2|+\ln\det|1-\tilde{t}g(\mathbf{k})|\}+\sum_i x_i\{\ln\det|1-(t_i-\tilde{t})\tilde{G}^{00}|+\ln\det|C_i(E)-iS_i(E)|\} , \tag{A5}$$

where the first determinant is taken for reciprocal lattice vectors $\mathbf{g}$'s, the rest are for angular momentum representations. Here $C_l(E)$ and $S_l(E)$ are the functions which are proportional to $\sin\eta_l$ and $\cos\eta_l$, respectively, but normalized such as to satisfy

$$\tilde{J}_l(r,E)=C_l(E)j_l(\sqrt{E}r)-S_l(E)n_l(\sqrt{E}r) , \tag{A6}$$

outside the muffin-tin sphere, where $\tilde{J}_l$ is the radial wave function normalized within an arbitrary (but fixed) sphere, e.g., the muffin-tin sphere. Such a normalization of $S(E)$ and $C(E)$ makes the analytic continuation of $Z(E)$ to the upper complex half plane of the physical-energy sheet possible; the procedure removes all the singularities which $\exp(-i\eta_l)=\cos\eta_l(E)-i\sin\eta_l(E)$ may have on the upper half plain at resonances of the single-site scattering (a similar method to eliminate the singularities was introduced by Drittler *et al.*[38] in total-energy calculations of impurity systems).

The band energy is now calculated by integrating $Z(E)$ with respect to E up to the Fermi level:

$$E_{\text{band}}=-\mathcal{I}\left\{Z(E_F)E_F-\int_{-\infty}^{E_F}Z(E)dE\right\} . \tag{A7}$$

We subtract from the band energy the potential energy

$$E_{\text{pot}}=\int_0^{r_{\text{mt}}}r^2dr\sum_i x_i\rho_i(r)v_i(r) , \tag{A8}$$

which is the configuration average of the expectation value of the single-site potential v_i at atom i, in order to obtain the kinetic energy of the noninteracting system in the sense of LSD. Here ρ_i is the electron density inside the muffin-tin sphere of atom i. The electrostatic energy E_{stat} (per atom, in atomic units) is obtained after Janak[39] as

$$E_{\text{stat}}=\sum_i x_i\left\{32\pi^2\int_0^{r_{\text{mt}}}dr\,r\rho_i(r)\int_0^r dr'r'^2\rho_i(r')-8\pi Q_i\int_0^{r_{\text{mt}}}r\rho_i(r)dr\right\}-\frac{1}{2}C\frac{Q_{\text{out}}^2}{a} , \tag{A9}$$

where a is the lattice constant, r_{mt} the muffin-tin radius; the constant C depending on the crystal structure is given in the table by Janak[39] as $C=4.832\,066\,4$, 4.085 521, and 3.116 685 7 for fcc, bcc, and sc lattice, respectively. Q_i in this expression is the nuclear charge of atom i and Q_{out} is the number of electrons per atom accumulated at the interstitial region, i.e.,

$$Q_{\text{out}}=\sum_i x_i\left\{Q_i-\int_0^{r_{\text{mt}}}r^2dr\,\rho_i(r)\right\} . \tag{A10}$$

The exchange-correlation energy (per atom) is given by the LSD approximation as

$$E_{\text{xc}}=\sum_i x_i\int_0^{r_{\text{mt}}}r^2dr\,\rho_i(r)\epsilon_{\text{xc}}(\rho_i)+Q_{\text{out}}\epsilon_{\text{xc}}(\rho_{\text{out}}) , \tag{A11}$$

where ϵ_{xc} is the exchange-correlation energy suitable for the homogeneous electron gas. All the core contributions should be included in the above expression.

[1] M. F. Collins and J. B. Forsyth, Philos. Mag. **8**, 401 (1963).
[2] J. Kanamori, H. Akai, N. Hamada, and H. Miwa, Physica **91B**, 153 (1976).
[3] T. Jo, J. Phys. Soc. Jpn. **50**, 2209 (1981).
[4] T. Jo, J. Phys. Soc. Jpn. **40**, 715 (1976).
[5] T. Jo and H. Miwa, J. Phys. Soc. Jpn. **40**, 706 (1976).
[6] H. Hasegawa and J. Kanamori, J. Phys. Soc. Jpn. **31**, 382 (1971); **33**, 1599 (1972); **33**, 1607 (1972).
[7] W. Kohn and L. J. Sham, Phys. Rev. **140**, A1133 (1965).
[8] L. Hedin and B. I. Lundqvist, J. Phys. C **4**, 2064 (1971).
[9] Y. Kitaoka and K. Asayama, J. Phys. Soc. Jpn. **40**, 1521 (1976).
[10] Y. Kitaoka, K. Ueno, and K. Asayama, J. Phys. Soc. Jpn. **45**, 142 (1978).
[11] J. Kanamori, Y. Teraoka, and T. Jo, in *Magnetism and Magnetic Materials—1974 (San Francisco),* Proceedings of the 20th Annual Conference on Magnetism and Magnetic Materials, edited by C. D. Graham, G. H. Lander, and J. J. Rhyne, AIP Conf. Proc. No. 24 (AIP, New York, 1975), p. 16.
[12] F. Ducastelle, J. Phys. **8**, 3297 (1975).
[13] For KKR-CPA-LSD, see, e.g., H. Akai, J. Phys. Condens. Matter **1**, 8045 (1989).
[14] D. D. Koelling and B. N. Harmons, J. Phys. C **10**, 3107 (1977).
[15] T. Takeda, Z. Phys. B **32**, 43 (1978).
[16] U. von Barth and L. Hedin, J. Phys. **5**, C 1629 (1972).
[17] V. L. Moruzzi, J. F. Janak, and A. R. Williams, *Calculated Electronic Properties of Metals* (Pergamon, New York, 1978).
[18] S. H. Vosko, L. Wilk, and M. Nusair, Can. J. Phys. **58**, 1200 (1980).
[19] Y. Ishikawa, R. Tournier, and J. Filippi, J. Phys. Chem. Solids **26**, 1727 (1965).
[20] J. O. Strom-Olsen, D. F. Wilford, S. K. Burke, and B. D. Rainford, J. Phys. F **9**, L95 (1979).
[21] B. Babic, F. Kajzar, and G. Parette, J. Phys. Chem. Solids **41**, 1303 (1980).
[22] S. K. Burke and B. D. Rainford, J. Phys. F **13**, 441 (1983); **13**, 471 (1983).

[23]S. K. Burke, R. Cywinski, J. R. Davis, and B. D. Rainford, J. Phys. F **13**, 451 (1983).
[24]T. Jo, J. Phys. Soc. Jpn. **51**, 794 (1982).
[25]H. Akai, S. Blügel, R. Zeller, and P. H. Dederichs, Phys. Rev. Lett. **56**, 2407 (1986).
[26]H. Akai, P. H. Dederichs, and J. Kanamori, J. Phys. (Paris) Colloq. **49**, C8-23 (1988).
[27]P. H. Dederichs, R. Zeller, H. Akai, and H. Ebert, J. Magn. Magn. Mater. **100**, 241 (1991).
[28]See, e.g., S. Blügel, H. Akai, R. Zeller, and P. H. Dederichs, Phys. Rev. B **35**, 3271 (1987).
[29]J. Kanamori and Y. Teraoka, J. Magn. Magn. Mater. **10**, 217 (1979).
[30]H. Hasegawa, J. Phys. Soc. Jpn. **46**, 1504 (1979).
[31]J. Hubbard, Phys. Rev. Lett. **B19**, 2626 (1979).
[32]T. Oguchi, K. Terakura, and N. Hamada, J. Phys. F **13**, 145 (1983).
[33]A. J. Pindor, J. Staunton, G. M. Stocks, and H. Winter, J. Phys. F **13**, 979 (1983).
[34]R. J. Weiss, Proc. Phys. Soc. London **82**, 281 (1963).
[35]H. Tange, T. Tokunaga, and M. Goto, J. Phys. Soc. Jpn. **45**, 105 (1978).
[36]H. Yamagata and M. Matsumura, J. Magn. Magn. Mater. **31-34**, 65 (1983).
[37]T. Jo and H. Akai, J. Phys. Soc. Jpn. **50**, 70 (1981).
[38]B. Drittler, M. Weinert, R. Zeller, and P. H. Dederichs, Phys. Rev. B **39**, 930 (1989).
[39]J. F. Janak, Phys. Rev. B **9**, 3985 (1974).